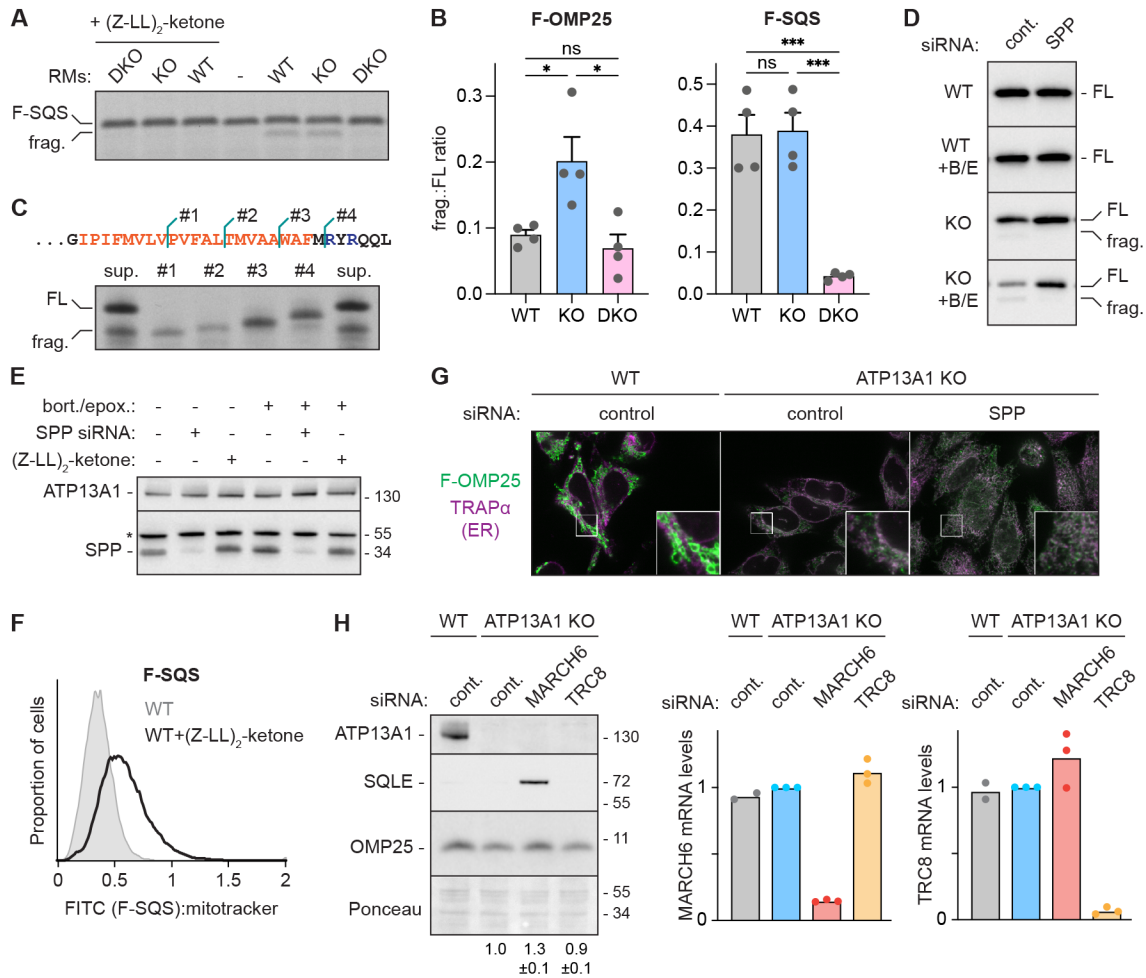


**Figure S1. The EMC is responsible for mitochondrial TA protein mislocalization** (related to Figure 1).

- (A)** ER insertase knockdown efficiencies. SDS-PAGE and immunoblotting for the indicated factors in wildtype (WT) and ATP13A1 knockout (KO) cells treated with control (cont.) siRNAs or siRNAs against EMC2, EMC6, or GET1.
- (B)** EMC depletion increases F-OMP25 mitochondrial localization. Immunofluorescence (left) of F-OMP25 (green) and the mitochondrial marker TOM20 (magenta) in WT or ATP13A1 KO Flp-In HeLa T-REx cells treated with cont. siRNAs or siRNAs against EMC2 or EMC6 (KD). Scale bar, 10  $\mu$ m. Bottom insets show magnified views of boxed region of F-OMP25 (green dot; left panels) or TOM20 (magenta dot, right panels). Manders' correlation coefficients (MCC; mean  $\pm$  sd and individual points for indicated sample size) measuring the colocalization of F-OMP25 and TOM20 (right). \*\*\*\*,  $p < 0.0001$ .

- (C)** The EMC mediates mislocalization of the mitochondrial TA protein BAK1. Pearson's correlation coefficients (PCC; mean  $\pm$  sd and individual points for indicated sample size) measuring colocalization of F-BAK1 and the ER marker TRAP $\alpha$  in WT or ATP13A1 KO cells treated with control siRNAs or siRNAs to knock down EMC2, EMC6, or GET1. \*\*\*\*,  $p < 0.0001$ ; ns, not significant.
- (D)** The EMC mediates mislocalization of the mitochondrial TA protein MAVS. Fluorescence microscopy of GFP-tagged OMP25 (GFP-OMP25; green; left) or MAVS (GFP-MAVS; green; right) cotransfected with a BFP ER marker (SS-BFP-KDEL; magenta) containing the BiP signal sequence and a KDEL ER retention sequence in WT, ATP13A1 KO, or ATP13A1 and EMC6 double knockout (DKO) cells.
- (E)** TA proteins annotated to be localized to the outer mitochondrial membrane (mito.; above axis), to both mitochondria and ER (on axis), or to the ER (below axis) sorted by increasing TM hydrophobicity (left to right) with the predicted  $\Delta G$  (kcal/mol) of membrane insertion indicated. C-terminal sequences of TA proteins analyzed in this study are shown with TM regions in orange.
- (F)** Characterization of ER-derived rough microsomes (RMs) from WT, ATP13A1 KO, or ATP13A1 and EMC6 DKO cells by SDS-PAGE and immunoblotting (left) and a long exposure of the samples in Figure 1C (right) showing a lower molecular weight F-OMP25 fragment (blue arrowhead) in the tot. and sup. fractions of insertion reactions with ATP13A1 KO RMs.



**Figure S2. SPP mediates mislocalized mitochondrial TA protein degradation** (related to Figure 2).

- (A)** SQS is cleaved by SPP. SDS-PAGE and autoradiography of radiolabeled F-SQS, a Flag-tagged TA protein reporter containing the squalene synthase TM sequence, in insertion reactions containing ER-derived rough microsomes (RMs) isolated from WT, ATP13A1 knockout (KO), or ATP13A1 and EMC6 double knockout (DKO) Flp-In 293 T-Rex cells without or with the SPP inhibitor (Z-LL)<sub>2</sub>-ketone. Note the F-SQS fragment (frag.) with WT and ATP13A1 KO RMs which is not generated with ATP13A1 and EMC6 DKO RMs or if (Z-LL)<sub>2</sub>-ketone is included.
- (B)** F-OMP25 is preferentially cleaved in the absence of ATP13A1. The ratio of the fragment (frag.) to full-length (FL) populations of F-OMP25 (left) or F-SQS (right) from *in vitro* insertion reactions with WT, ATP13A1 KO, and ATP13A1 and EMC6 DKO RMs normalized to values obtained with WT RMs (mean + sem and individual values shown) for 3 replicates. \*\*\*,  $p < 0.001$ ; \*,  $p < 0.05$ .
- (C)** Cleavage occurs within the F-OMP25 TM. C-terminal F-OMP25 sequence (top) and autoradiography (bottom) of anti-Flag immunoprecipitations of soluble (sup.) radiolabeled F-OMP25 from insertion reactions with RMs isolated from ATP13A1 KO cells, or of radiolabeled F-OMP25 truncated at the points indicated in the sequence (#1-#4). The OMP25 TM is underlined. FL – full-length F-OMP25; frag. – F-OMP25 fragment whose size falls between the products produced by the #1 and #2 truncation sites.

- (D)** SPP-dependent cleavage of mislocalized F-OMP25. SDS-PAGE and immunoblotting of F-OMP25 in WT or ATP13A1 KO cells treated with control (cont.) siRNAs or siRNAs to knock down SPP followed by treatment with proteasomal inhibitors (0.5  $\mu$ M bortezomib + 0.5  $\mu$ M epoxomicin; B/E) as indicated. The F-OMP25 fragment is only apparent in ATP13A1 KO cells, enhanced upon proteasome inhibition, and suppressed by knocking down SPP.
- (E)** SPP inhibition does not change SPP levels. SDS-PAGE and immunoblotting of ATP13A1 and SPP in WT cells treated without or with bort./epox., siRNAs against SPP, and/or 5  $\mu$ M (Z-LL)<sub>2</sub>-ketone. \*, non-specific band.
- (F)** SPP regulates SQS abundance. Fluorescent flow cytometry of WT cells expressing a FLAG-tagged reporter TA protein containing the squalene synthase TM (F-SQS) and treated without (gray) or with (Z-LL)<sub>2</sub>-ketone (black), confirming F-SQS as an SPP client. F-SQS levels assayed by staining with FITC-labeled anti-FLAG antibodies were normalized to mitotracker staining.
- (G)** SPP inhibition stabilizes mislocalized F-OMP25 at the ER in ATP13A1 KO cells. Immunofluorescence of F-OMP25 (green) and the ER marker TRAP $\alpha$  (magenta) in WT and ATP13A1 KO Flp-In HeLa T-REx cells treated with control siRNAs or siRNAs targeting SPP. Scale bar, 10  $\mu$ m.
- (H)** Role of MARCH6 in mislocalized OMP25 ERAD. Immunoblotting for the indicated factors in WT or ATP13A1 KO cells treated with control (cont.) siRNAs or siRNAs to knock down MARCH6 or TRC8 (left). SQLE – squalene monooxygenase, a known ERAD client of MARCH6. Owing to the lack of reliable antibodies, knockdown efficiencies of MARCH6 (middle) and TRC8 (right) were assayed by RT-qPCR. Shown are mean and individual values of 2-3 replicates normalized to ATP13A1 KO cells treated with cont. siRNAs.

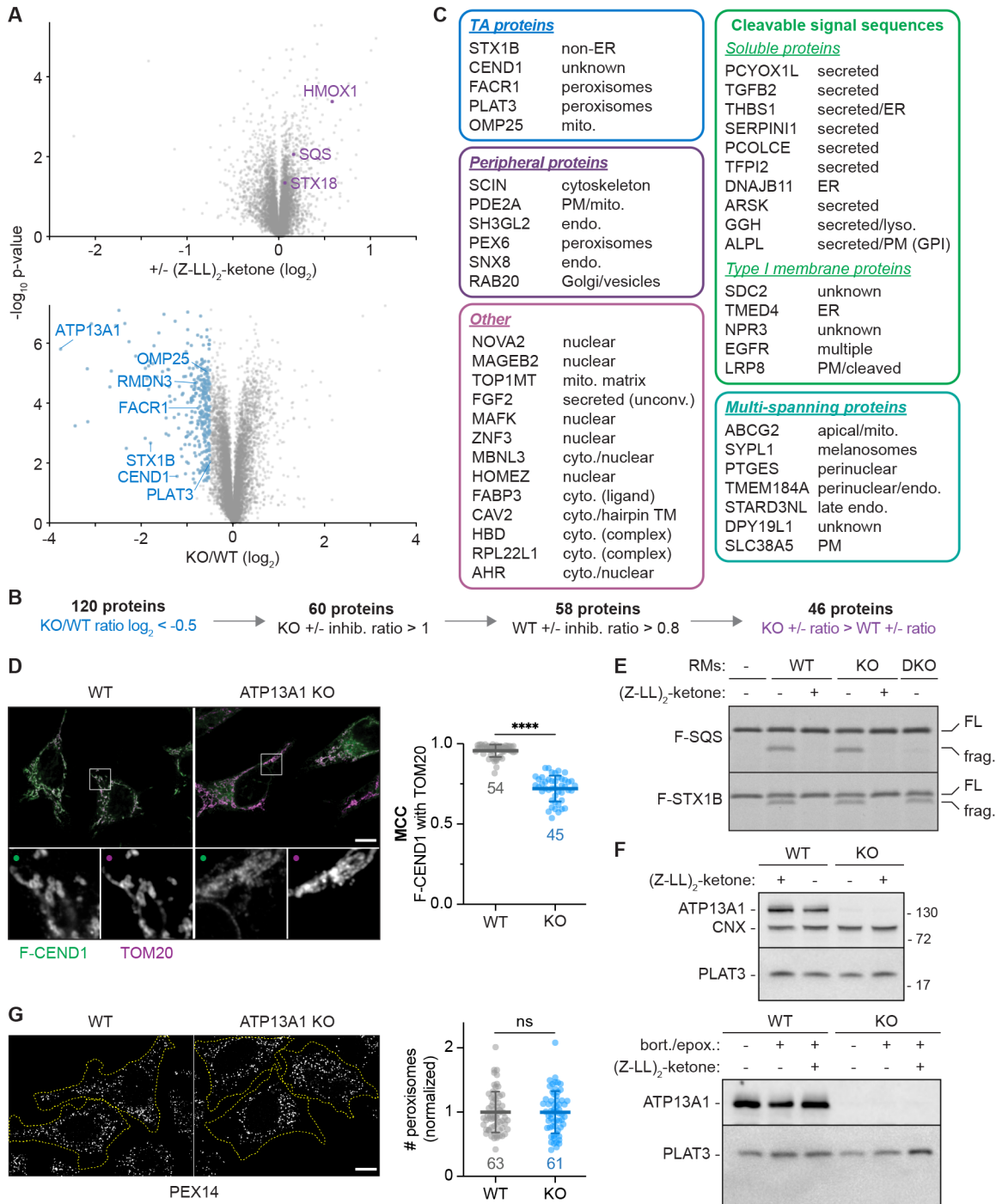


**Figure S3. Quantitative proteomics to identify clients regulated by ATP13A1 and SPP** (related to Figure 2).

- (A)** Proteome-wide effects of depleting ATP13A1 and inhibiting SPP. Volcano plots showing relation of  $\log_2$  fold change and p-value of protein levels in wildtype (WT) cells treated with and without (Z-LL)<sub>2</sub>-ketone (top) or ATP13A1 knockout (KO) compared to WT cells (bottom). Proteins with decreased abundances in ATP13A1 KO cells (blue) were filtered to identify proteins stabilized by SPP inhibition. Known SPP clients are shown in purple.
- (B)** Filtering for proteins whose abundances are influenced by both ATP13A1 and SPP.

- (C) Classification and annotated cellular localization of proteins from (B).
- (D) CEND1 is a mitochondrial TA protein. Immunofluorescence (left) and Manders' correlation coefficients (MCC; right; mean  $\pm$  sd and individual points for indicated sample size) showing colocalization of a FLAG-tagged reporter containing the CEND1 TM (F-CEND1; green) and the mitochondrial marker TOM20 (magenta) in WT or ATP13A1 KO Flp-In HeLa T-REx cells. Scale bar, 10  $\mu$ m; \*\*\*\*,  $p < 0.0001$ .
- (E) Validation of TA proteins cleaved by SPP. SDS-PAGE and autoradiography of radiolabeled FLAG-tagged reporters containing the SQS (top; F-SQS) or STX1B (bottom; F-STX1B) TM were synthesized *in vitro* and incubated without (-) or with rough microsomes (RMs) isolated from WT, ATP13A1 KO, or ATP13A1 and EMC6 double knockout (DKO) cells in the absence or presence of (Z-LL)<sub>2</sub>-ketone. Full-length (FL) and cleaved (frag.) clients are indicated. Unlike F-OMP25, F-SQS and F-STX1B are cleaved equally well in WT and ATP13A1 KO RMs, and F-STX1B is not significantly affected by knocking out EMC6.
- (F) SDS-PAGE and immunoblotting for endogenous PLAT3 in WT and ATP13A1 KO cells treated without or with (Z-LL)<sub>2</sub>-ketone and/or the proteasome inhibitors bortezomib and epoxomicin (bort./epox.).
- (G) Immunofluorescence of the peroxisomal marker PEX14 in WT and ATP13A1 KO cells with cells outlined by yellow dotted line (left), and quantification of the number of peroxisomes per cell per field of view, normalized to the mean of WT samples (right). Shown are mean  $\pm$  sd and individual points for indicated sample size. Scale bar, 10  $\mu$ m.

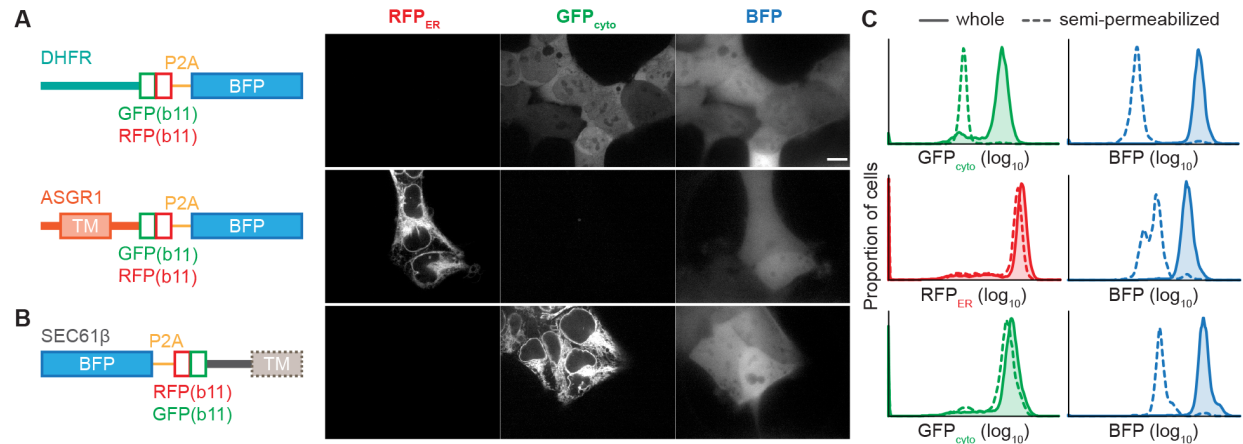


**Figure S4. Validation of an ER membrane protein topology reporter system** (related to Figure 3).

- (A)** Reporter protein scheme (left) and fluorescence microscopy (right) showing RFP<sub>ER</sub>, GFP<sub>cyto</sub>, and BFP signal in cells expressing the indicated topology reporters as in Figure 3A. Scale bar, 10  $\mu$ m.
- (B)** As in (A) but with a reporter (left) of the ER-targeted TA protein SEC61 $\beta$ . Because SEC61 $\beta$  is a tail-anchored protein with a C-terminal ER-targeting TM, the order of the BFP, P2A sequence, and tandem b11 tag was reversed and placed at the N-terminus.
- (C)** Fluorescent flow cytometry showing RFP<sub>ER</sub>, GFP<sub>cyto</sub>, or BFP signal of whole (solid) or semi-permeabilized (dotted) cells expressing the indicated reporter. Note: soluble GFP<sub>cyto</sub> and BFP signals decrease upon semi-permeabilization while RFP and GFP signals of membrane-embedded reporters persist after semi-permeabilization.



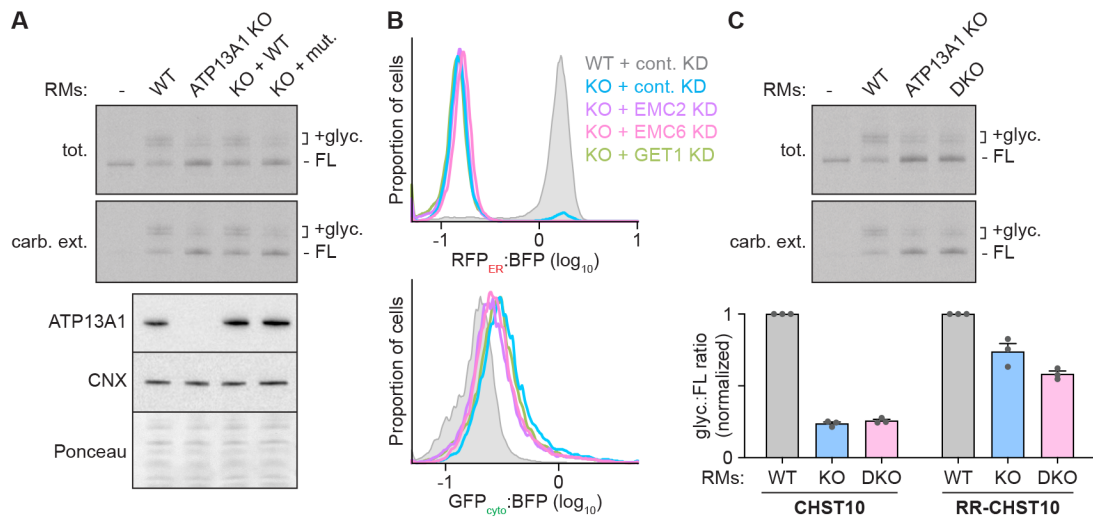


**Figure S5. Contributions to CHST10 topogenesis** (related to Figure 4).

- (A)** CHST10 topogenesis is ATP13A1-dependent. SDS-PAGE and autoradiography (top) of radiolabeled CHST10 synthesized *in vitro* without or with ER-derived rough microsomes (RMs) isolated from wildtype (WT), ATP13A1 KO, or ATP13A1 KO cells re-expressing WT or catalytically inactive (D533A; mut.) ATP13A1 before (tot.) or after carbonate extraction (carb. ext.). FL, full-length substrate; +glyc, glycosylated substrate populations. Representative of 3 experiments quantified in Figure 4C. RMs used in the reactions were also analyzed by SDS-PAGE and immunoblotting (bottom).
- (B)** EMC depletion does not alter CHST10 topogenesis. RFP<sub>ER</sub>:BFP (top) and GFP<sub>cyto</sub>:BFP (bottom) ratios of CHST10 reporters expressed in WT (gray) or ATP13A1 KO cells treated with control (cont.) siRNAs or siRNAs against EMC2, EMC6, or GET1.
- (C)** SDS-PAGE and autoradiography (top) of insertion reactions of radiolabeled CHST10 without or with RMs isolated from WT, ATP13A1 KO, or ATP13A1 and EMC6 double-knockout (DKO) cells. Ratios of glycosylated to full-length (glyc.:FL) CHST10 and RR-CHST10 in insertion reactions with the indicated RMs were quantified for 3 independent reactions and normalized to reactions with WT RMs (mean + sem; bottom).



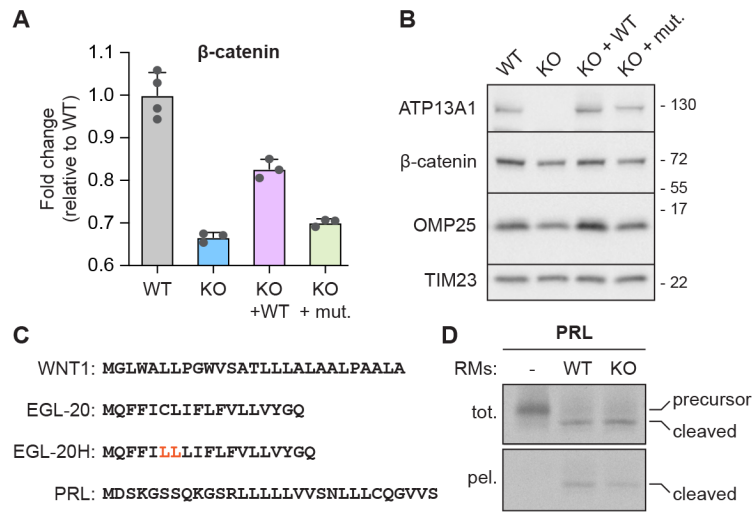


**Figure S6. ATP13A1-dependent signal sequences** (related to Figure 5).

- (A) Endogenous  $\beta$ -catenin levels measured by multiplexed quantitative mass spectrometry (McKenna et al., 2020) in wildtype (WT), ATP13A1 knockout (KO), or KO Flp-In HeLa T-REx cells re-expressing WT ATP13A1 or catalytically inactive (D533A; mut.) ATP13A1, normalized to WT levels.
- (B) Immunoblotting for the indicated proteins in WT, ATP13A1 KO, KO + WT, and KO + mut. cells showing ATP13A1-dependent stabilization of  $\beta$ -catenin and OMP25.
- (C) Signal sequences of human WNT1, its *C. elegans* homolog EGL-20, an EGL-20 mutant that is more hydrophobic (EGL-20H), and bovine preprolactin (PRL).
- (D) SDS-PAGE and autoradiography of denaturing immunoprecipitations of radiolabeled PRL with a C-terminal FLAG tag synthesized *in vitro* without or with ER-derived rough microsomes (RMs) isolated from WT or ATP13A1 KO cells before (tot.) or after pelleting (pel.) to enrich RM-associated populations. Precursor and signal-cleaved substrates are indicated.

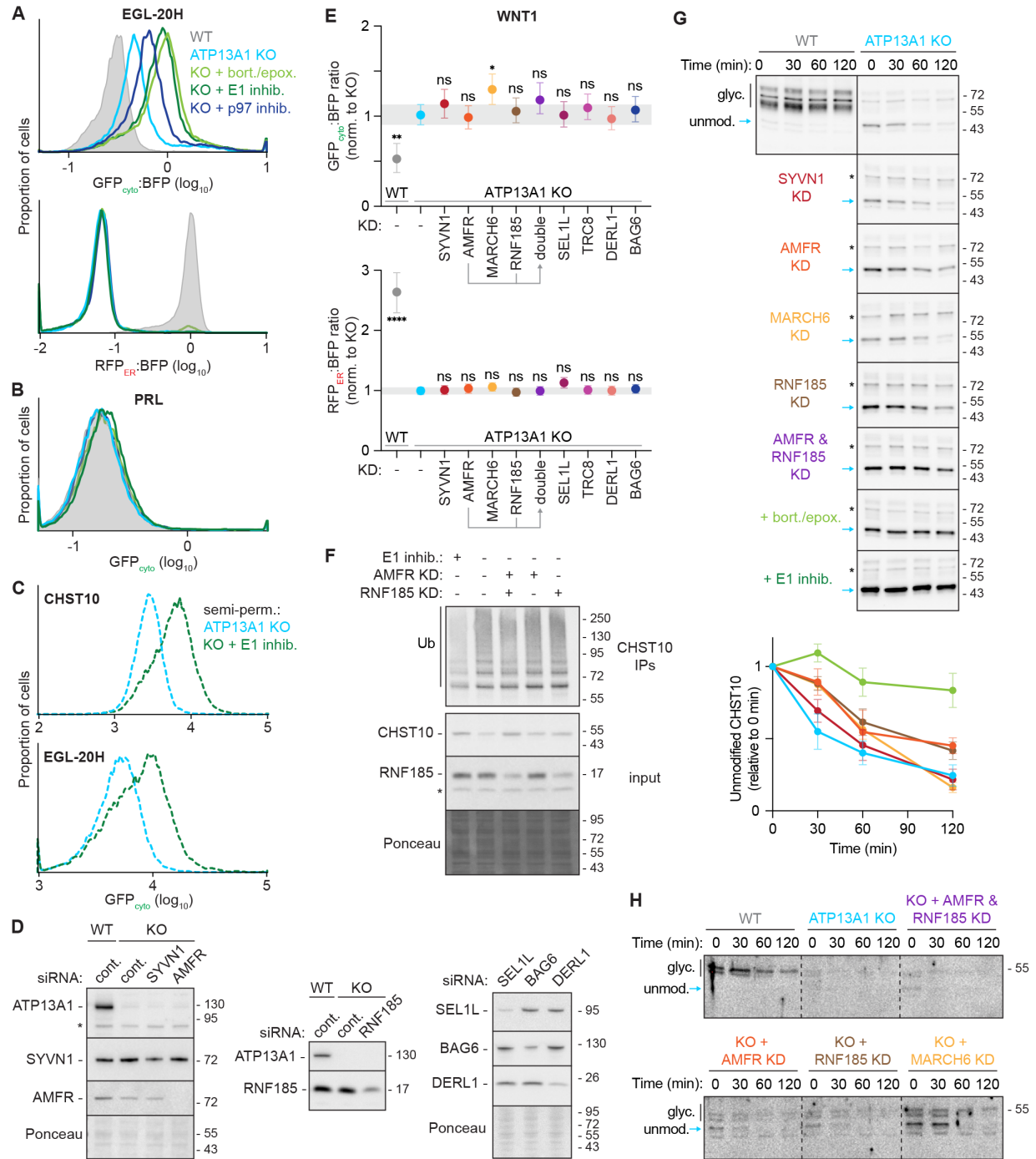


**Figure S7. ERAD of misoriented proteins** (related to Figure 6).

**(A)** GFP<sub>cyto</sub>:BFP (top) and RFP<sub>ER</sub>:BFP (bottom) ratios of the EGL-20H signal sequence topology reporter in wildtype (WT; gray) or ATP13A1 knockout (KO) cells treated without (light blue) or with inhibitors (inhib.) of proteasomal activity (0.5 μM bortezomib and 0.5 μM epoxomicin; bort./epox.; light green), the E1 ubiquitin activating enzyme (1 μM MLN7243; dark green), or the p97 AAA-ATPase (1 μM CB-5083; dark blue). The WT and KO RFP<sub>ER</sub>:BFP ratios are the same as in Figure 5A.

- (B)** GFP<sub>cyto</sub>:BFP ratios of the PRL signal sequence topology reporter in WT cells treated with control (gray) or siRNAs to knock down (KD) ATP13A1 treated without (light blue) or with inhibitors against the ubiquitin-proteasome system as in (A).
- (C)** GFP<sub>cyto</sub> levels of semi-permeabilized ATP13A1 KO cells expressing the CHST10 type II (top) or EGL-20H signal sequence (bottom) topology reporter treated without (light blue) or with (dark green) 1  $\mu$ M MLN7423 for 4 hr to inhibit the E1 ubiquitin activating enzyme.
- (D)** Ubiquitin ligase knockdown efficiencies assayed by SDS-PAGE and immunoblotting for the indicated factors in WT or ATP13A1 KO cells treated with control (cont.) siRNAs or siRNAs to knock down the indicated factors.
- (E)** ERAD factors involved in misoriented WNT1 ERAD. GFP<sub>cyto</sub>:BFP (top) and RFP<sub>ER</sub>:BFP (bottom) ratios of the WNT1 topology reporter in WT (gray) or ATP13A1 KO cells treated with control (-) siRNAs (light blue) or siRNAs to knock down (KD) the indicated factors. Shown are median values and interquartile range of at least two biological replicates of  $n \geq 6,000$  each. \*\*,  $p < 0.01$ ; \*,  $p < 0.05$ .
- (F)** Misoriented CHST10 ubiquitination decreases with AMFR and RNF185 depletion. Immunoprecipitations (IPs; top) of the CHST10 topology reporter from lysates of ATP13A1 KO cells treated without or with E1 inhibitor or siRNAs to knock down (KD) AMFR and/or RNF185 were analyzed with input lysates (bottom) by SDS-PAGE and immunoblotting for cotransfected HA-tagged ubiquitin or the indicated factors. Note: unmodified CHST10 levels increase but ubiquitination levels decrease when AMFR and RNF185 are knocked down at the same time, similar to E1 inhibition.
- (G)** Timecourse of misoriented CHST10 ERAD. Translation shut-off reactions were initiated with the addition of 50  $\mu$ g/mL cycloheximide to WT or ATP13A1 KO cells expressing the CHST10 type II topology reporter treated with control siRNAs (light blue) or siRNAs to knock down (KD) the indicated factor(s), proteasome inhibitors (bort./epox.; light green), or E1 inhibitor (dark green). Samples taken at the indicated timepoints were analyzed by immunoblotting (top). Unmodified CHST10 intensities were quantified, normalized to time = 0 min, and plotted (bottom). Shown are mean  $\pm$  sem for 3 replicates.
- (H)** Timecourse of misoriented WNT1 ERAD. Translation shut-off reactions as in (G) in WT or ATP13A1 KO cells expressing the WNT1 signal sequence topology reporter treated with control siRNAs (light blue) or siRNAs against the indicated factor(s). Samples taken at the indicated timepoints were analyzed by immunoblotting.